JP2.20 LOCATING AND REMOVING PROBLEMATIC DATA IN THE DMSP SSM/I DATA SETS

Andrew L. Molthan* and Mark R. Anderson
University of Nebraska-Lincoln, Lincoln, NE

1. INTRODUCTION

Snow cover and sea ice in the polar regions are believed to have a dominant role in the regional and global surface energy balance due to their seasonal and annual variability that result in a sharp change in surface albedo. Due to the hostile polar environment, standard surface or upper air observations are difficult to perform and maintain, therefore remote sensing platforms and algorithms have been developed to monitor both current conditions and changes over time at the poles. For example, passive microwave brightness temperatures have been used to determine sea ice concentrations (i.e. Cavalieri et al. 1991, Comiso et al. 1986) as well as melt onset (i.e. Belchansky et al. 2004, Drobot and Anderson 2001, Smith 2001), melt out and freeze-up conditions (i.e. Parkinson 1992) over the Arctic Ocean. These data have also been used with atmospheric data to investigate interactions between the surface and atmosphere (i.e. Drobot and Anderson 2002**,** Cavalieri and Parkinson 1987).

2. DATA

Daily 25 km resolution grids of passive microwave brightness temperatures generated by the Special Sensor Microwave Imager (SSM/I) onboard the Defense Meteorological Satellite Program (DMSP) platforms F8 (1987-91), F11 (1991-1995) and F13 (1996 to present) were obtained on CD-ROM from the National Snow and Ice Data Center (NSIDC). Four frequencies (85.5, 37.0, 22.2 and 19.3 GHz) are available with three of the channels (85.5, 37.0 and 19.3 GHz) in horizontal and vertical polarizations. The daily gridded SSM/I products are formulated by taking the orbital SSM/I antenna temperatures, converting them to brightness temperatures and gridding them into a polar stereographic projection (Fig. 1) using the 'drop in the bucket' sum and average method (Maslanik and Stroeve 2004).

3. OBSERVATIONS

Improved technology, software and computer storage capacity allows for daily plotting of brightness temperatures for individual channels. Analysis of the daily gridded data revealed arcs of brightness temperatures that varied significantly from adjacent and surrounding pixels. These arcs of inconsistent brightness temperatures will be referred to as "bad scans" from this point forward.

Corresponding author address: Andrew L. Molthan, Meteorology/Climatology Program, Dept of Geosciences, 214 Bessey Hall, Lincoln, NE 68588-0340, e-mail: amolthan@papagayo.unl.edu

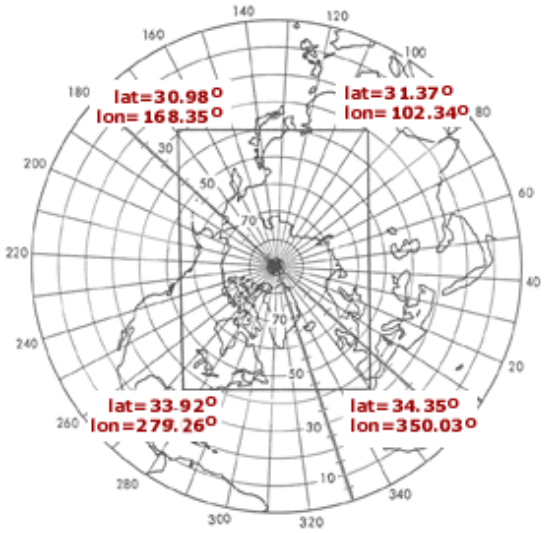

FIG. 1. Northern Hemisphere coverage area of the daily average 25 km resolution DMSP SSM/I brightness temperatures. Image courtesy of NSIDC.

Examples of these bad scans are shown for horizontally and vertically polarized 19.3 and 37.0 GHz channels, and the vertically polarized 22.2 GHz channel in Fig. 2. Incorrect values included in the daily brightness temperature grids can have drastic effects on the results of any algorithm that exploits channel differences. For example, the Advanced Horizontal Range Algorithm (AHRA, Drobot and Anderson 2001) makes decisions regarding melt onset by evaluating channel differences and bad scans in one or more channels create local melt date anomalies. The NASA Team ice concentration algorithm (Cavalieri et al. 1991) also employs channel differencing and ratios in order to calculate total and multiyear ice fractions. Depending on the magnitude of error in the individual bad scans and whether or not the bad scans are collocated in multiple channels, the derived ice concentration may vary significantly in a bad scan region. When only the 19.3 GHz channel is contaminated with a bad scan the difference in total or multiyear ice concentration between good and bad pixels is around 5% but when multiple channels are affected the difference in concentration approaches 20% (Fig. 3).

A bad scan detection algorithm was created to locate bad scan pixels based on pixel to pixel differences in time and space. The algorithm exploits the concept that brightness temperatures do not vary greatly unless in a transition period from large changes in emissivity or physical temperature. This routine was most successful when working with the 19.3 GHz horizontal polarization (19H) and is used here to evaluate and describe the shape, size and impacts of individual bad scans.

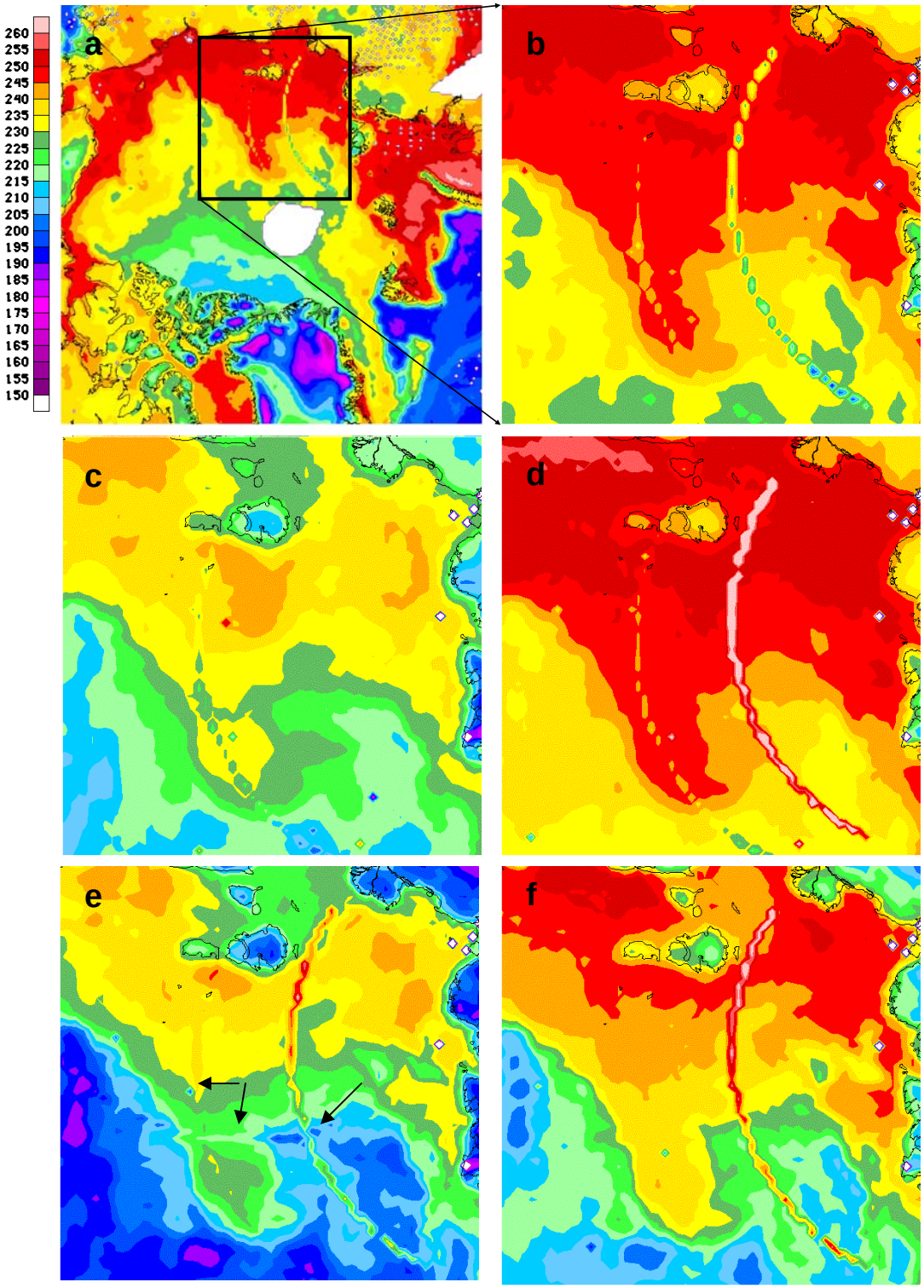

FIG. 2. Fields of brightness temperatures for 21 March 1989 (K) for the following channels: (a) vertically polarized 22.3 GHz brightness temperatures for much of the Arctic as well as a box indicating the subset region used for figures b-e (b) subset of the vertically polarized 22.3 GHz, (c) horizontally polarized 19.3 GHz, (d) vertically polarized 19.3 GHz, (e) horizontally polarized 37.0 GHz , and (f) vertically polarized 37.0 GHz for 21 March 1989. Bad scans are the arc shaped discontinuities of values and colors aligned top towards bottom. The arrows in (e) point to the approximate centers of the three bad scans in the 37H channel. For scale, the island top and center in each figure is Novosibirskiye in the Laptev Sea. Some smoothing of values in the gradient takes place between the bad scans and adjacent pixel values.

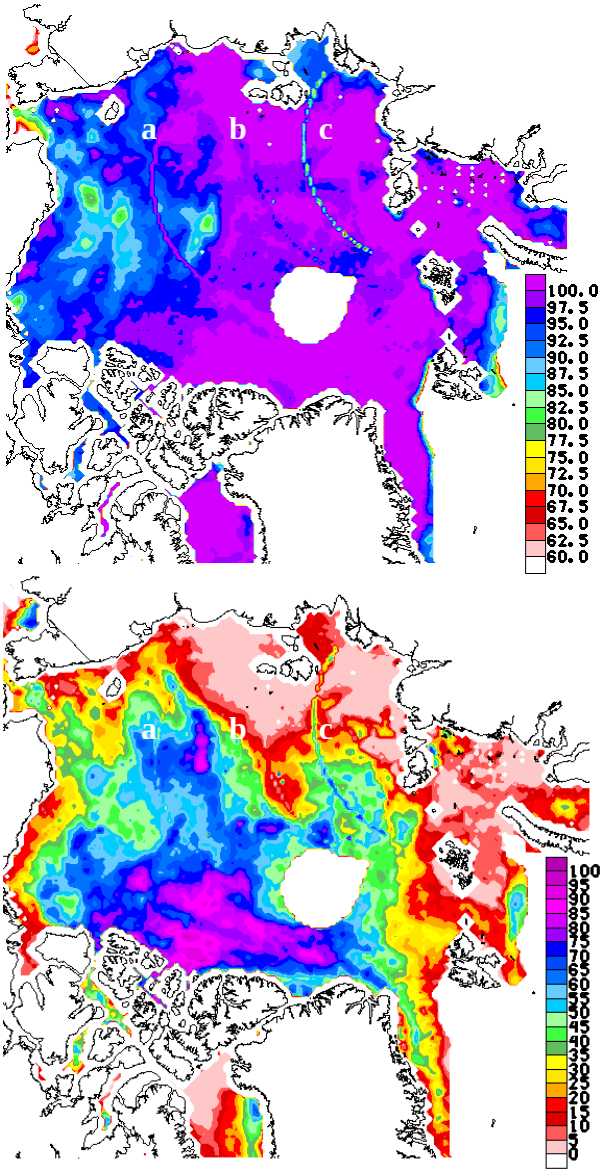

FIG. 3. Ice concentrations derived with the NASA Team Algorithm for 21 March 1989. Top: Total ice concentration (%) with three bad scan areas well defined near locations (a)-(c). These values are derived using the brightness temperatures shown in Fig. 2. Bottom: Multiyear ice concentration (%, note scale difference) with similar bad scan arcs. Arc (a) in both concentration fields is the result of bad scans that fall outside of the subset region in Fig. 2.

3. RESULTS

The bad scan detection algorithm was run daily for 1 March through 30 September 1989. Verification of the algorithm was completed by comparing detected bad scans against brightness temperature fields. In some cases, the routine was unable to detect complete scans from beginning to end but instead detected sizable sections of them with some discontinuities. A count of all bad scans detected including full length scans detected by the routine and scans that were incomplete or broken was completed for the 19H and horizontally polarized 37.0 GHz (37H) channels. The 19H channel had 67 days with at least one bad scan while the 37H data contained 51 contaminated days. Those totals are 28% and 21% of the 19H and 37H days investigated, respectively. A compilation of all continuous bad scans detected by the routine and believed to be in the 19H or 37H channels was completed (Fig. 4). Bad scans may occur in multiple channels on the same day, and although unlikely, they may also be collocated or partially overlapping.

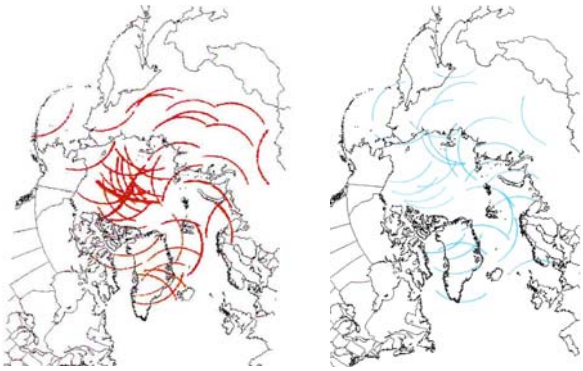

FIG. 4. Composite map indicating locations of bad scans determined by the algorithm for the 19H (red, left) and 37H (blue, right) brightness temperature fields from 1 March 1989 to 30 September 1989.

A sample of ten individual scans that were identified by visual inspection and the bad scan detection algorithm were also examined. In these ten cases, the detection routine located the bad scans although omitted pixels were included by hand in order to complete the scan length. Adding pixels to the scan length or filling in gaps is somewhat subjective. The influence of the bad scan is apparent by tracking inconsistencies in brightness temperatures where the detection routine failed. From the small sample of ten bad scans, pixel length ranged from 57 to 62 with an average of 60. An individual bad scan was usually one or two pixels wide. Magnitude differences between bad scan brightness temperature points and adjacent points typically ranged from 5 to 15 K, although individual points approached 20 K differences (see Fig. 2). Actual values for the 19H, location of bad scan points and derived parameters are displayed for a small subset in Figure 5.

4. SUMMARY AND CONCLUSIONS

Data inconsistencies were located in the daily averaged DMSP SSM/I brightness temperatures for the F8, F11 and F13 platforms. Inconsistent values occur in scan-shaped patterns in individual channels, are not necessarily collocated in multiple channels and appear randomly over the open water, ice or land areas in the SSM/I coverage grid. While the Northern Hemisphere coverage area was the only area investigated there is no reason to assume that the Southern Hemisphere is error free.

Algorithms and routines used to track changes in polar regions that are sensitive to channel differences or individual channels in the DMSP SSM/I daily gridded

0	1	1	1	1	1
0	0	1	1	1	1
1	0	1	1	1	1
1	1	0	1	1	1
1	1	1	0	1	1
1	1	1	1	0	1
1	1	1	1	1	0
1	1	1	1	1	0

223.9	231.5	231.2	230.1	229.0	228.2
226.6	223.0	230.7	229.8	229.0	228.9
230.3	225.4	230.2	229.4	228.2	228.9
229.5	230.3	222.5	229.2	228.0	227.6
227.1	227.6	228.3	216.9	226.0	225.2
223.9	223.4	225.2	224.1	217.8	223.9
220.0	220.5	222.0	221.1	221.6	216.3
217.5	218.9	218.9	219.0	219.5	213.7

94	99	100	100	99	100
96	94	99	99	99	99
98	96	98	99	98	99
99	99	96	99	99	100
99	98	99	94	99	98
99	98	98	99	96	99
100	100	100	100	99	97
100	100	100	100	99	96

0	14	19	21	25	32
9	3	23	25	29	30
22	8	21	23	28	27
21	20	8	27	36	31
29	28	21	15	38	32
47	43	35	43	30	37
60	58	44	47	46	36
64	62	56	58	54	41

FIG. 5. Subset values along and in the vicinity of a bad scan in the 19H channel on 21 March 1989. From top to bottom: binary result of bad scan detection algorithm where a value of zero indicates a bad scan pixel, actual brightness temperatures (K) for the 19H channel, total ice concentration derived with the NASA Team Algorithm (%) and multiyear ice concentration (%). Color filled boxes indicate the location of bad scan pixels in the 19H brightness temperatures.

brightness temperatures are affected by the bad scans currently present in the NSIDC data set. Although the effect of bad scans on individual days may be small, the cumulative effect of bad scans over multiple days or in small subset regions may be significant.

Contact with NSIDC revealed that these bad scans are result from at least two errors: "bad" data that were not flagged prior to the drop in the bucket averaging or differences in the gridding routines used before 2000 (Stroeve 2004, personal communication). The problem of bad scans in data for years 1988 to 2000 is being addressed by regridding the data using the system employed for data sets for 2001 and beyond. Users of the data should update their sources with the newly gridded versions as soon as they become available and check previous results for potential errors. Reprocessing of the data sets containing bad scans began in October of 2004 and is expected to take six months to complete and will be available from NSIDC.

5. REFERENCES

Belchansky, G. I., Douglas, D. C., Platonov, N. G.. 2004: Duration of the Arctic Sea Ice Melt Season: Regional and Interannual Variability, 1979–2001. J. Climate, 17, 67–80.

Cavalieri, D.J. and C.L. Parkinson. 1987: On the relationship between atmospheric circulation and sea-ice fluctuations in the sea-ice extents of the Bering and Okhotsk Seas. J. of Geophys. Res., 92, 7141-7162.

Cavalieri, D. J., J. Crawford, M. R. Drinkwater, D. Eppler, L. D. Farmer, R. R. Jentz and C. C. Wackerman. 1991: Aircraft active and passive microwave validation of sea ice concentration from the DMSP SSM/I. J. Geophys. Res., 96, 21,989-22,009.

Comiso, J. C. 1986: Characteristics of Arctic winter sea ice from satellite multispectral microwave observations. J. Geophys. Res., 91, 975-994.

Drobot, S.D., and M.R. Anderson, 2001: An improved method for determining snowmelt onset dates over Arctic sea ice using scanning multichannel microwave radiometer and Special Sensor Microwave/Imager data. J. Geophys. Res., 106, 24,033-24,050.

Drobot, S.D., and M.R. Anderson, 2001: Comparison of interannual snowmelt-onset dates with atmospheric conditions. Ann. Glaciology. 33, 79-81.

Parkinson, C.L. 1992: Spatial patterns of increases and decreases in the length of the sea ice season in the north polar region. J. Geophys. Res., 97, 14,377-14,388.

Smith, D.M. 1998: Observation of perennial Arctic sea ice melt and freeze-up using passive microwave data. J. Geophys. Res., 103, 27,753-27,769.

Maslanik, J., and J. Stroeve. 2004: DMSP SSM/I daily polar gridded brightness temperatures, 1988 to 2003. Boulder, CO: National Snow and Ice Data Center. CD-ROM.